

Periodic index separate confinement heterostructure InGaAs/AlGaAs multiple quantum well laser grown by organometallic vapor phase epitaxy

W. S. Hobson, M. C. Wu, Y. K. Chen, and M. A. Chin
AT&T Bell Laboratories, Murray Hill, New Jersey 07974

M. Geva
AT&T Bell Laboratories, Breinigsville, Pennsylvania 18031

K. S. Jones
University of Florida, Gainesville, Florida 32611

(Received 28 October 1991; accepted for publication 16 November 1991)

Organometallic vapor phase epitaxy was used to grow a novel periodic index separate confinement heterostructure (PINSCH) InGaAs/AlGaAs multiple quantum well (MQW) laser. Secondary ion mass spectrometry and transmission electron microscopy were used to characterize the structure. The performance of the PINSCH laser was compared with that of a graded index separate confinement heterostructure (GRINSCH) MQW laser grown under similar conditions. The PINSCH laser uses cladding layers comprised of periodic semiconductor multilayers ($\text{Al}_{0.4}\text{Ga}_{0.6}\text{As}/\text{GaAs}$) which provide both optical and electrical confinement. Since the optical field decays over several multilayers, and therefore is far less tightly confined than in the GRINSCH structure, a significant reduction of the transverse far-field angle occurs. Comparing the performance of $5 \times 750 \mu\text{m}$ self-aligned ridge waveguide InGaAs/AlGaAs lasers emitting at 980 nm, the PINSCH structure exhibits a transverse far-field angle of 23° compared to 46° for the GRINSCH. This is obtained at the expense of a modest increase in threshold current (19 mA vs 10 mA).

There has been significant recent interest in high power InGaAs/AlGaAs quantum well lasers emitting at 980 nm for use as the pump source for erbium-doped fiber amplifiers.¹ A particularly important laser parameter is the optical beam divergence since this governs the fraction of emitted power which can be effectively coupled into the fiber. Graded-index separate confinement heterostructure (GRINSCH) lasers have resulted in the lowest thresholds and highest external differential quantum efficiencies.^{2,3} However, GRINSCH lasers typically exhibit large (e.g., 50°) transverse far-field angles due to the tight transverse optical confinement provided by the graded AlGaAs layers. Previous approaches to decreasing the optical confinement have included large optical cavity (LOC) laser structures.^{4,5} However, thresholds are higher for LOC lasers due to the weak optical and electrical carrier confinement.

Recently, a new device structure, the periodic index separate confinement heterostructure (PINSCH), has been applied to 980 nm InGaAs/AlGaAs quantum well lasers.⁶ The cladding layers consist of alternating layers of $\text{Al}_{0.4}\text{Ga}_{0.6}\text{As}$ and GaAs which provide both optical and electrical carrier confinement. The transverse optical confinement is expanded over that of the GRINSCH laser since approximately three $\text{Al}_{0.4}\text{Ga}_{0.6}\text{As}/\text{GaAs}$ periods are required until the optical field decays. In addition to the reduced transverse beam divergence resulting from the larger optical cavity, higher output powers prior to catastrophic optical damage should be attainable since the power density at the laser facet is reduced. The theoretical basis of the PINSCH laser structure has been discussed previously.⁶

In order to successfully grow the PINSCH structure excellent control over layer thickness is required. Previously, molecular beam epitaxy was used as the growth technique.⁷ A novel growth procedure was employed, whereby the Al and Ga furnace temperatures were ramped in order to grade layers and the growth took place at 600°C in order to accurately control the layer thickness. (OMVPE) should be well suited to the growth of these structures due to its excellent thickness control, long term reproducibility, high optical quality of AlGaAs, and the capability to grow AlGaAs at high temperatures without difficulty in controlling the composition. This latter point is particularly important since higher growth temperatures are desirable for the growth of the highest quality AlGaAs.

Here, we report on OMVPE growth, characterization, and performance of a PINSCH laser structure. Secondary ion mass spectrometry (SIMS) and transmission electron microscopy (TEM) were used to characterize the layer structure. The performance of the PINSCH and GRINSCH lasers (ridge-waveguide structure) is compared. The transverse far-field angle of the PINSCH laser is reduced to 23° compared to the GRINSCH value (46°). There is a modest increase of threshold current (19 mA vs 10 mA).

A custom-built OMVPE reactor operated at atmospheric pressure was used for the growth of the PINSCH and GRINSCH laser structures. The design is similar to that described by Matsumoto *et al.*⁸ and consists of a vertical-geometry reactor with an upstream quartz flow modifier which can be adjusted in a predictable manner to provide a uniform flow velocity across the 2 in. diam wafer. The small upstream reactor volume and the laminar nature of the flow ensure a rapid exchange of reactants above the

TABLE I. Epitaxial layer structure of PINSCH MQW laser.

Layer composition	Thickness (nm)	Doping concentration ($p, n: 10^{18} \text{ cm}^{-3}$)
GaAs	200	$p=10$
$\text{Al}_{0.4}\text{Ga}_{0.6}\text{As}/\text{GaAs}$, 8 period SL	145	$p=0.6$
$\text{Al}_{0.4}\text{Ga}_{0.6}\text{As}$	145	$p=0.6$
GaAs	44	$p=0.6$
GaAs	40	undoped
$\text{In}_{0.2}\text{Ga}_{0.8}\text{As}/\text{GaAs}$, MQW active layer	7/20	undoped
GaAs	40	undoped
GaAs	44	$n=1.0$
$\text{Al}_{0.4}\text{Ga}_{0.6}\text{As}/\text{GaAs}$, 8 period SL	145	$n=1.0$
$\text{Al}_{0.4}\text{Ga}_{0.6}\text{As}$	145	$n=1.0$
$\text{GaAs}/\text{Al}_{0.4}\text{Ga}_{0.6}\text{As}$, 5 period SL	10/10	$n=3.0$
GaAs	500	$n=3.0$

wafer. A fast switching radial manifold with pressure-balanced vent/run lines is used. The rotation rate of the wafer was 30 rpm. Trimethylgallium, trimethylaluminum, and trimethylindium were used as the gallium, aluminum, and indium sources, respectively. Arsine was used as the arsenic source at a partial pressure of 3 Torr. Diethylzinc and disilane were used as the Zn and Si dopant precursors. The GaAs growth rate was kept constant at 27 nm min^{-1} . The structures were grown at 700°C except for the InGaAs/GaAs multiple quantum well (MQW) active layer which was grown at 625°C . A growth interruption was used prior to and after the growth of the MQW active in order to allow time for the temperature change.

The PINSCH structure is given in Table I. Abrupt AlGaAs/GaAs interfaces and moderate p -type doping (mid 10^{17} cm^{-3}) were used for this first attempt. The comparison GRINSCH structure consists of the same active region and uses the same basic growth procedure. The $\text{Al}_x\text{Ga}_{1-x}\text{As}$ is graded from $x = 0.0$ to $x = 0.4$ over a distance of 185 nm on each side of the active layer of the

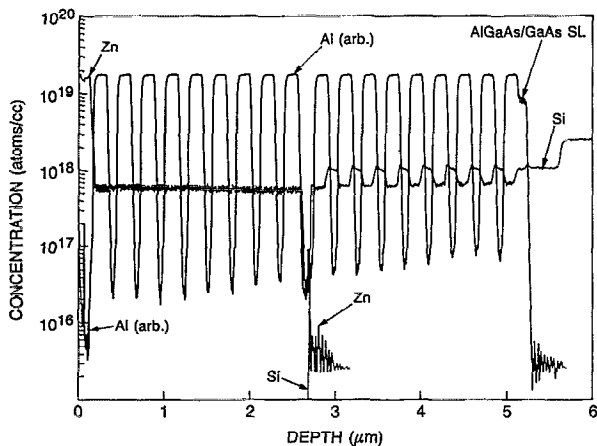


FIG. 1. SIMS profiles of the atomic Al, Zn, and Si concentrations in the PINSCH MQW laser structure.

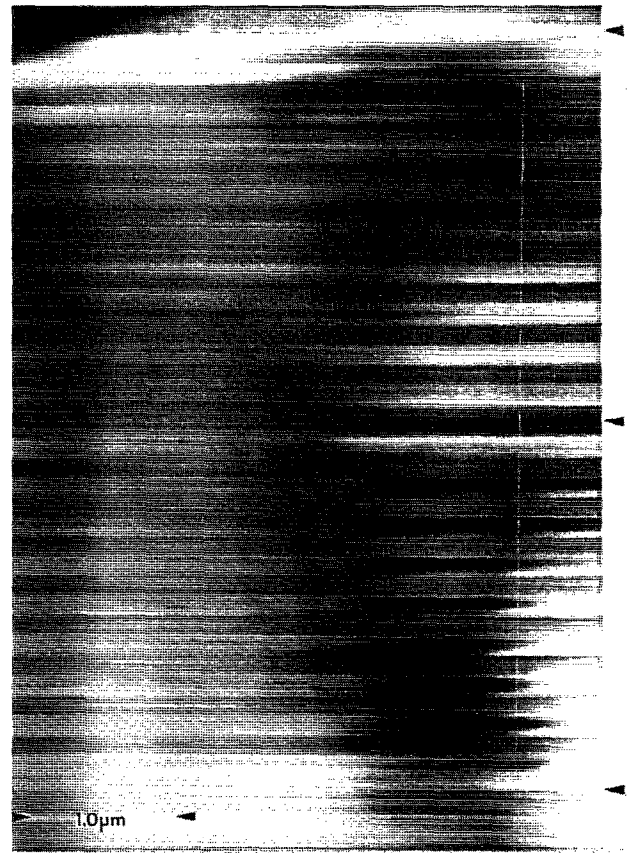


FIG. 2. TEM micrograph of the entire PINSCH MQW laser structure.

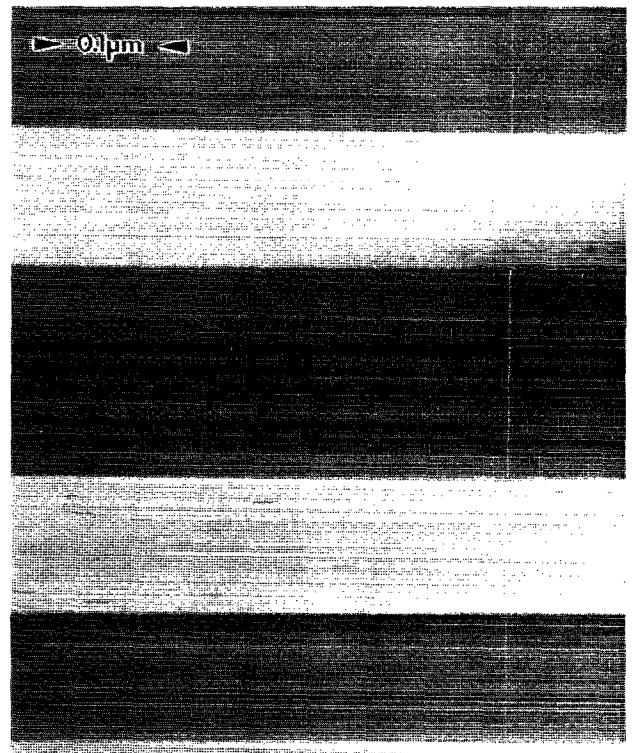


FIG. 3. TEM micrograph of the MQW active region of the PINSCH MQW laser structure, with one set of the AlGaAs/GaAs layers shown.

GRINSCH laser, and the $\text{Al}_{0.4}\text{Ga}_{0.6}\text{As}$ cladding layers are $1.3\ \mu\text{m}$ thick.

The PINSCH MQW layer structure was characterized by a CAMECA IMS-4f SIMS instrument and atomic concentration profiles of Al, Si, Zn, C, and O were obtained. The SIMS atomic concentration depth profiles of Al, Si, and Zn are given in Fig. 1. One notes the excellent layer-to-layer reproducibility of the Al profile. The Zn profile exhibits an abrupt falloff in the active layer. The Si doping in the GaAs layer is higher than in the $\text{Al}_{0.4}\text{Ga}_{0.6}\text{As}$ layer ($1.3 \times 10^{18}\ \text{cm}^{-3}$ vs $7 \times 10^{17}\ \text{cm}^{-3}$) and reflects the higher growth rate of AlGaAs while the Si dopant flow was held constant. Since the resistance of the *n*-cladding layer is quite low, the precise Si-doping layer is not of importance for the laser performance. The carbon concentration (not shown) in the $\text{Al}_{0.4}\text{Ga}_{0.6}\text{As}$ layers was $6 \times 10^{16}\ \text{cm}^{-3}$. The oxygen concentration in the $\text{Al}_{0.4}\text{Ga}_{0.6}\text{As}:\text{Zn}$ was $1.5 \times 10^{17}\ \text{cm}^{-3}$, while it was slightly higher ($2.5 \times 10^{17}\ \text{cm}^{-3}$) in $\text{Al}_{0.4}\text{Ga}_{0.6}\text{As}:\text{Si}$. This may be due to $\text{H}_2\text{O}/\text{O}_2$ contamination of the disilane source since no *in situ* purifier was used on this particular line. Nevertheless, the oxygen background throughout the structure is relatively low based on a comparison with AlGaAs which was grown in other reactors, using either OMVPE or MBE, when examined on the same SIMS instrument. These oxygen values are also low when compared with literature values,⁹ with the exception of the use of trimethylamine alane as the aluminum source.¹⁰ As expected, the carbon and oxygen concentrations in the GaAs layers and InGaAs/GaAs active region were below the detection limits of the SIMS instrument.

A TEM micrograph of the full PINSCH laser structure is shown in Fig. 2, with the beginning of the AlGaAs/GaAs buffer SL layer, the center of the InGaAs/GaAs MQW active layer, and the top *p*⁺ GaAs contact layer marked at the right. The micrograph was taken on a JEOL 200 CX scanning transmission electron microscope using the g_{200} reflection and centered dark-field imaging conditions. One notes the excellent layer-to-layer thickness repeatability and overall high structural quality of the sample. An expanded view of the InGaAs/GaAs active layer and one set of the adjacent AlGaAs/GaAs layers (only part of the top GaAs layer appears) is shown in Fig. 3. The MQW active region exhibits very high quality InGaAs/GaAs layers with no evidence of structural defects.

Ridge-waveguide PINSCH and GRINSCH lasers were fabricated using a self-aligned process reported previously. Wet chemical etching was used to form the $5\text{-}\mu\text{m}$ -wide (measured at the ridge base) ridge waveguide. Polyimide was used to planarize the structure.

The room-temperature continuous-wave (CW) light-versus-current curve of the PINSCH laser is given in Fig. 4. A threshold current of $J_{\text{th}} = 19\ \text{mA}$ was obtained, which was moderately higher than that of the GRINSCH laser ($J_{\text{th}} = 10\ \text{mA}$) for the same dimensions. The transverse far-field angle (θ_T) was 23° for the PINSCH laser which

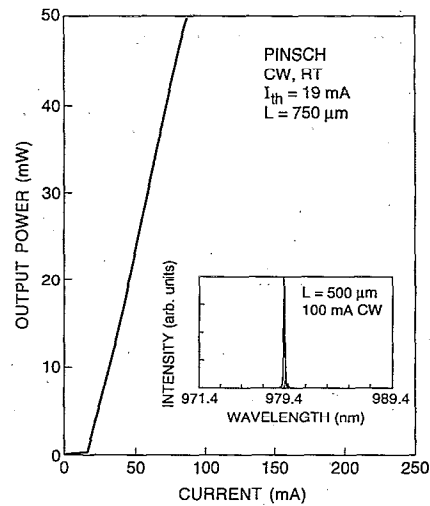


FIG. 4. The room-temperature CW *L-I* curve of a $5\ \mu\text{m} \times 750\ \mu\text{m}$ PINSCH laser; the inset shows the laser emission spectrum from a $5\ \mu\text{m} \times 500\ \mu\text{m}$ laser.

represents a significant reduction compared to the GRINSCH laser ($\theta_T = 46^\circ$). The emission spectrum for a PINSCH laser with a $500\ \mu\text{m}$ cavity length is shown in the inset of Fig. 4. Single transverse mode operation at $\sim 980\ \text{nm}$ was obtained until $100\ \text{mA}$ drive current, at which point higher order modes also become apparent. Further optimization of the ridge waveguide (e.g., reduced width at the ridge base) will suppress the higher order modes.

In summary, we have used OMVPE to grow a novel PINSCH InGaAs/AlGaAs MQW laser structure. The PINSCH laser exhibited a transverse far-field angle of 23° compared to 46° for a GRINSCH laser grown under similar conditions. This significant reduction of θ_T was obtained at the expense of a modest increase in threshold current ($J_{\text{th}} = 19\ \text{mA}$ vs $10\ \text{mA}$).

¹U. Uehara, M. Okayasu, T. Takeshita, O. Kogure, M. Yamada, M. Shimizu, and M. Horiguchi, *Optoelectronics* **5**, 71 (1990).

²H. K. Choi and C. A. Wang, *Appl. Phys. Lett.* **57**, 321 (1990).

³R. L. Williams, M. Dion, F. Chatenoud, and K. Dzurko, *Appl. Phys. Lett.* **58**, 1816 (1991).

⁴H. F. Lockwood, H. Kressel, H. S. Sommers, and F. Z. Hawrylo, *Appl. Phys. Lett.* **17**, 499 (1970).

⁵N. K. Dutta, J. Lopata, P. R. Berger, D. L. Sivco, and A. Y. Cho, *Electron. Lett.* **27**, 680 (1991).

⁶M. C. Wu, Y. K. Chen, M. Hong, J. P. Mannaerts, M. A. Chin, and A. M. Sergent, *Appl. Phys. Lett.* **59**, 1046 (1991).

⁷M. Hong, M. C. Wu, Y. K. Chen, J. P. Mannaerts, and M. A. Chin (unpublished).

⁸K. Matsumoto, K. Itoh, T. Tabuchi, and R. Tsunoda, *J. Cryst. Growth* **77**, 151 (1986).

⁹T. Achnick, G. Burri, and M. Ilegems, *J. Vac. Sci. Technol. A* **7**, 2537 (1989).

¹⁰W. S. Hobson, J. P. van der Ziel, A. F. J. Levi, J. O'Gorman, C. R. Abernathy, M. Geva, L. C. Luther, and V. Swaminathan, *J. Appl. Phys.* **70**, 432 (1991).